DOI 10.52209/2706-977X_2023_4_3 **IRSTI 53.49.19** **UDC 681.2.088**

Estimation of Temperature Effects on Uncertainties of Dimensional Measurements in Industrial Computed Tomography by Finite Element Modeling

Drégelyi-Kiss Á.*, Anh Dao Duy, Farkas G., Gonda V.
Óbuda University, Budapest, Hungary
*corresponding author

Abstract. Using industrial computed tomography (CT) in measuring dimensional parameters (such as diameter, distance) of manufactured parts becomes more and more popular due to its advantages such as being a non-destructive method and possibility to complete complex shape measurements rapidly. However, the accuracy and precision of the measured values are required to be validated by quality control. The complicated structure of multi-step processing contribute to measurement errors and uncertainties through various factors. Among them, temperature change during the operation of CT machine possesses a high potential influence. Two test geometries created in Catia V5 were modelled in Marc Mentat Finite Element software considering different materials (PMMA, Al, AlMgSi1) to study the deformation behavior against the change of temperature during the CT measurement process. The results of simulations provided an appropriate point of view about the effect of the temperature parameter to the measurement accuracy and uncertainties.

Keywords: dimensional metrology, CT measurements, measurement error, measurement uncertainty, finite element modeling, temperature effects.

Introduction

In modern industry, dimensional metrology is essential for quality control. Until now, optical and tactile systems have been popular because of their accuracy and the certificated uncertainties. However, for the purpose of evaluation the internal structure of a part or an assembly, these systems face real challenges.

In recent years, CT dimensional measurements have emerged as a solution to the difficulties of controlling the overall structure of the product [1]. Known as a non-destructive method, CT can map 2D, or 3D images of objects, which are directly processed by assistant software (such as VGS studio [2] to implement dimensional metrology's requirements, in a short time.

Notwithstanding, because of the complexity of CT systems and the measurement strategy, data traceability becomes extraordinarily difficult. Figure 1 introduces comprehensively factors influencing the performance of CT system in dimensional metrology [3,4].

Because there are variety of sources can contribute to measurement errors and uncertainties, research about them becomes essential and popular. About the impact of X-ray source, research about the effect of focal spot size, focus drift and tube power (including voltage, current) were implemented [5,6,7]. The influence of material, temperature and surface roughness of specimen were also investigated by several authors [8,9,10,11,12,13]. On the other hand, the detector contributes to measurement errors through main parameters such as detective quantum efficiency and image lag [5,14]. The step of image processing possibly affects to the accuracy of metrology measurement [15,17].

In 2015, an experiment implemented by H. Villarraga-Gomez [11,12], specimens with identical geometry but different material quality were measured by CT method, and studied the effect of external parameter influences for the accuracy of measurements. The temperature change at position of workpiece were also recorded. Features were measured at different stages of CT processing to determine the behavior of measurement uncertainties under the effect of temperature.

In this paper, two specimens with different structures were modelled in simulated to evaluate how the distribution of measurement errors caused by changing of temperature will be. Furthermore, the results of simulations were compared with the work of H. Villarraga-Gomez to compare the compensation of temperature change used in [11,12].

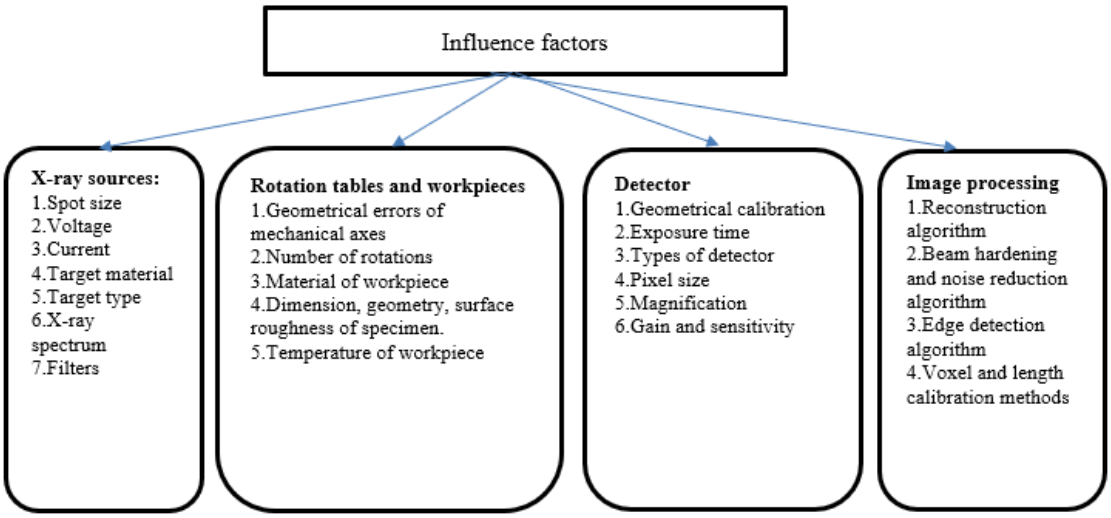

Fig. 1. – Influencing factors on dimensional metrology by CT

1. Materials and Methods

1.1 Theoretical background

Followed by the Guide to the Expression of Uncertainty in Measurement (GUM) (clause 3.2.4) [19] and with the assumption that the same application from ISO 15530 for tactile CMMs [20] was used for X-ray CT in measurement uncertainties estimation, the correct measurement result by CT system X_{corr} of n independent observations which has arithmetic mean $\bar{X}_{CT}$ can be calculated as follows:

$$X_{corr} = \bar{X}_{CT} - b \pm U_{CT} \tag{1}$$

where b is the bias of systematic errors calculated by the $\bar{X}_{CT}$ minus the true value (reference value) measured by a more accurate system than CT (CMMs). U_{CT} is equal to $k \cdot u_{CT}$ with k = 2 for confidence interval of 95% and u_{CT} is a quadratic sum of several basic contributions [18,20]:

$$u_{ct} \approx \sqrt{{u_{ref}}^2 + {u_p}^2 + {u_w}^2 + {u_b}^2} \tag{2}$$

where u_{ref} is the standard uncertainties of reference value or in certificated calibration procedure for the specimen. It is normally assumed that this value is negligible in comparison with other elements in (2). Parameter $u_p$is the uncertainty of repeatability and u_w is the variation as a consequence of expansion due to temperature change or surface roughness. As a component of u_w, the uncertainties in the temperature change is considered as the largest influence. It was calculated by the Eq. (3) [11,12]:

$$u_T \approx \beta L|\Delta T|/\sqrt{3} \tag{3}$$

where β is the expansion coefficient, L is the length of the measurand (in meter) and ΔT is the change of temperature projected to the reference temperature (20°C). Constant of $\sqrt{3}$ illustrates for the assumption of the rectangular error distribution for temperature. Finally, u_b is the standard uncertainty caused by systematic errors of the calibration measurement procedure includes two main contributors: deviation between CT measurement and reference values and the uncertainty due to thermal expansion for the calibrated workpiece. Generally, if systematic errors are compensated, Eq. (2) will be used. However, in case of being not fully compensated, the formula was proposed in ISO/TS 15530-3:2009 [20] will be used:

$$u_{ct} \approx \sqrt{{u_{ref}}^2 + {u_p}^2 + {u_w}^2 + b^2} \tag{4}$$

1.2 Materials and models

Two test geometries were defined for the analysis. The geometry of the first sample for this study was a rectangular block (referred hereafter as the 'hole block') with outer dimensions of 20 mm × 40 mm × 60 mm with a 10 mm diameter hole passing through the center of the longest axis (Figure 2a). The used materials for this geometry were poly(methyl methacrylate) (PMMA) and aluminum.

The second geometry was made of aluminum alloy (AlMgSi1). It has the shape of a cube with the size of 90 mm × 90 mm × 90 mm. In this block, 14 holes were defined with a distributed layout as in the Figure 1b. The physical parameters of materials are listed in Table 1.

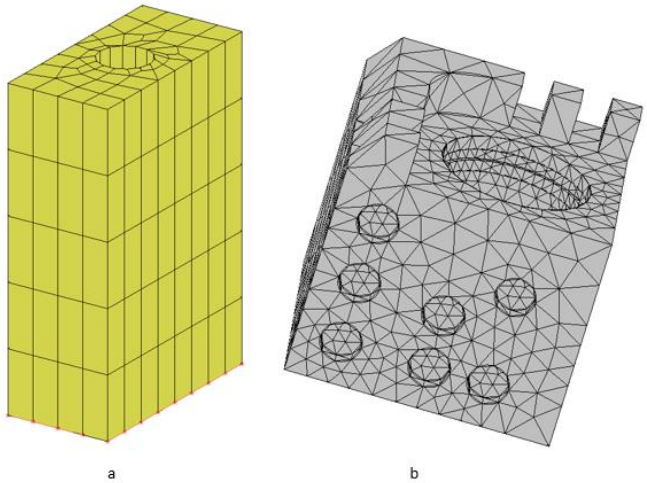

Fig. 2. – Test geometries with finite element mesh the first geometry (a), the second geometry (b).

Table 1. The parameters of materials

Type of parameters	***PMMA***	***Aluminum***	***AlMgSi1***
Mass density	$1.18\times10^{6}\ kg/m^{3}$	$2.7\times10^{6} kg/m^{3}$	$2.7\times10^{6}\ kg/m^{3}$
Thermal conductivity	$0.21\ Wm^{-1}K^{-1}$	$237\ Wm^{-1}K^{-1}$	$195\ Wm^{-1}K^{-1}$
Specific heat	$1466\ Jkg^{-1}K^{-1}$	$898.7\ Jkg^{-1}K^{-1}$	$900\ Jkg^{-1}K^{-1}$
Young modulus	2450 MPa	70 GPa	70 GPa
Poisson ratio	0.375	0.33	0.33
Thermal expansion	$126\ \mu m\ m^{-1}°C^{-1}$	$23.4\ \mu m\ m^{-1}°C^{-1}$	$23.4\ \mu m\ m^{-1}°C^{-1}$

2. Method

Finite element method (FEM) was employed in Marc Mentat, which is a popular method for solving problems of engineering and mathematical models. In FEM, geometry is divided into a large system of small, simpler parts called elements, which is implemented by the construction of a mesh of object. The simple equations modelling the finite one will be assembled into a larger system of equations modelling entire problem. Marc Mentat is a popular software could use FEM to handle with complicated issues [21]

There are several common parameters among simulations. Constraints for displacements are applied to 4 points at corners of the bottom of workpieces. The distribution of temperature is assumed to be uniform over the whole solid part. The varied parameter in this simulation was the temperature, temperature data were used as in [11,12]. There were 5 regions:

- Region 1: the warm up phase (X-ray was turned on) lasted 1-1.5 hour and temperature increased up to 22°C
- Region 2: the X-ray was turned off in 4.5-5h. Temperature decreases to 21.4°C at the end of phase.
- Region 3: X-ray was turned on to make measurement. The temperature raised to 22.15°C at the end of phase 3. This stage lasted 3 hours.
- Region 4: CT maintain active whole the region in 8 hours. The temperature reached the highest value during operation (22.45°C)
- Region 5: Power tube was turned off. The temperature went down to 21.9°C.

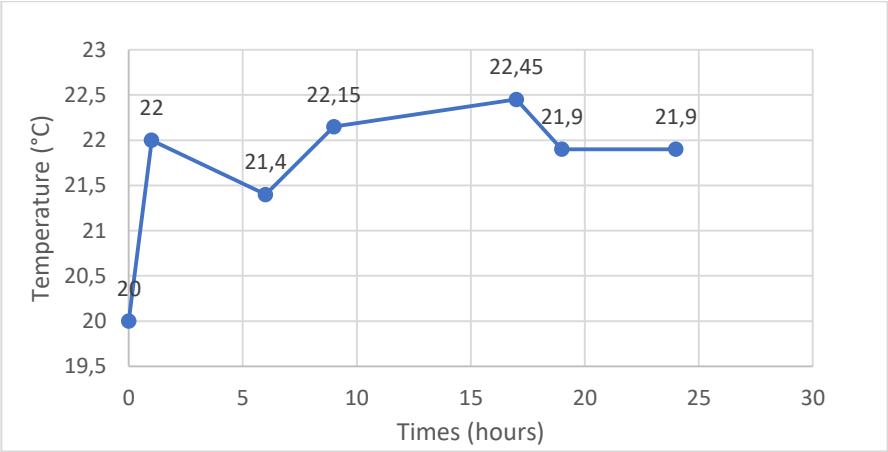

Fig. 2. – Graph of temperature change used in simulation

Fig. 3 illustrates the changes in temperature for each region. The simulation was divided in to 2 phases:

Phase 1: Using the information about temperature in Fig. 3 to simulate the behavior of two model under the effect of temperature change. From this phase, the distribution of displacement will be revealed. The maximum value of displacement will also be recorded.

Phase 2: At the end of region 5 the temperature decreased to 21.9°C which is the average temperature used in [11,12] for calculating the compensated value. The value in simulation at this temperature will be recorded and made comparison to evaluate if we can simply use Eq. (5) to calculate the corrected value:

$$\Delta l \approx \beta l \Delta T \tag{5}$$

The time for scanning by CT usually lasts several hours that is extremely long for simulation. Therefore, unit of hour was converted to second with respect ratio (1 hour was converted to 1 second in simulation)

Simulation results

Four types of results were extracted: displacement field in x,y,z-direction and the total displacement field displayed by vectors.

Table 2. Node has max value and max value of first model made of PMMA

	Node has max value of displacement	*Max value of displacement [μm]*
In x direction	1, 2	-6.29,6.28
In y direction	3, 4	3.751, -3.712
In z direction	5	22.44
Total displacement	5	23.47

Table 3. Node has max value and max value of first model made of Aluminum

	Node has max value of displacement	*Max value of displacement [μm]*
In x direction	1,2	-1.166, 1.165
In y direction	3,4	0.683, 0.677
In z direction	5	4.127
Total displacement	5	4.322

Table 4. Node has max value and max value of second model made of AlMgSi1

	Node has max value of displacement	*Max value of displacement [μm]*
In x direction	7,8	3.052, -2.785
In y direction	9,10	2.888, -2.591
In z direction	11	7.582
Total displacement	12	8.173

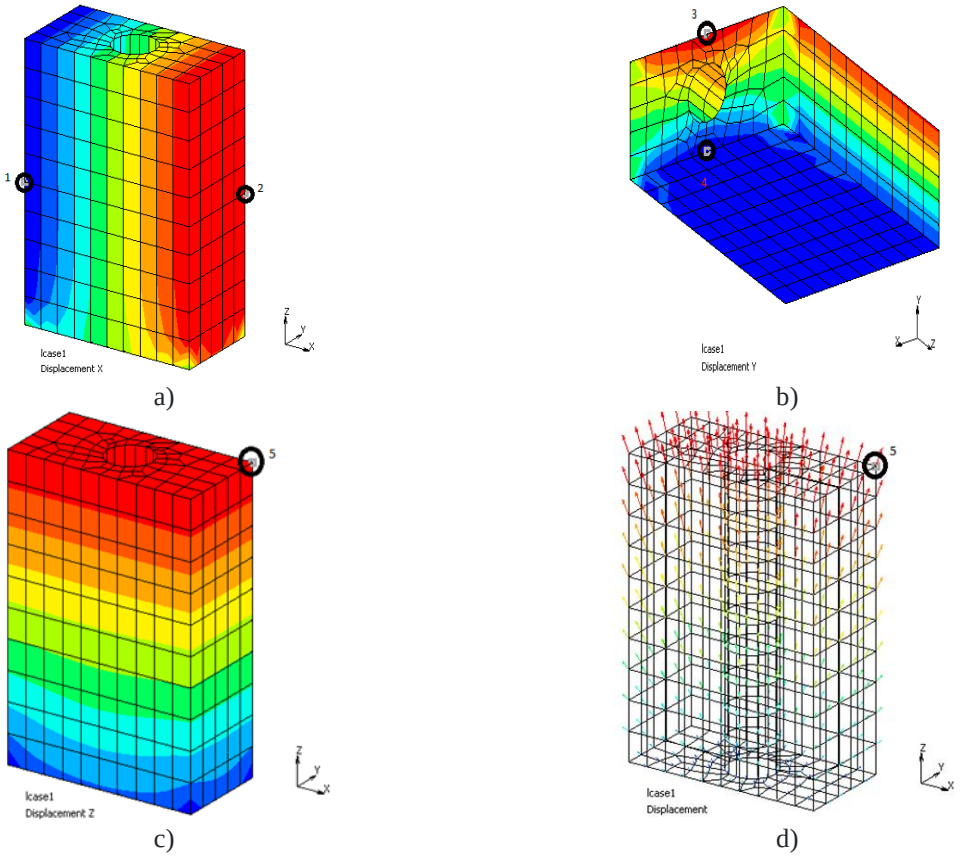

Fig. 3. – The displacement of the first model made of PMMA under simulation. a) x-direction, b) y-direction displacement, c) z-direction displacement, d) total displacement.

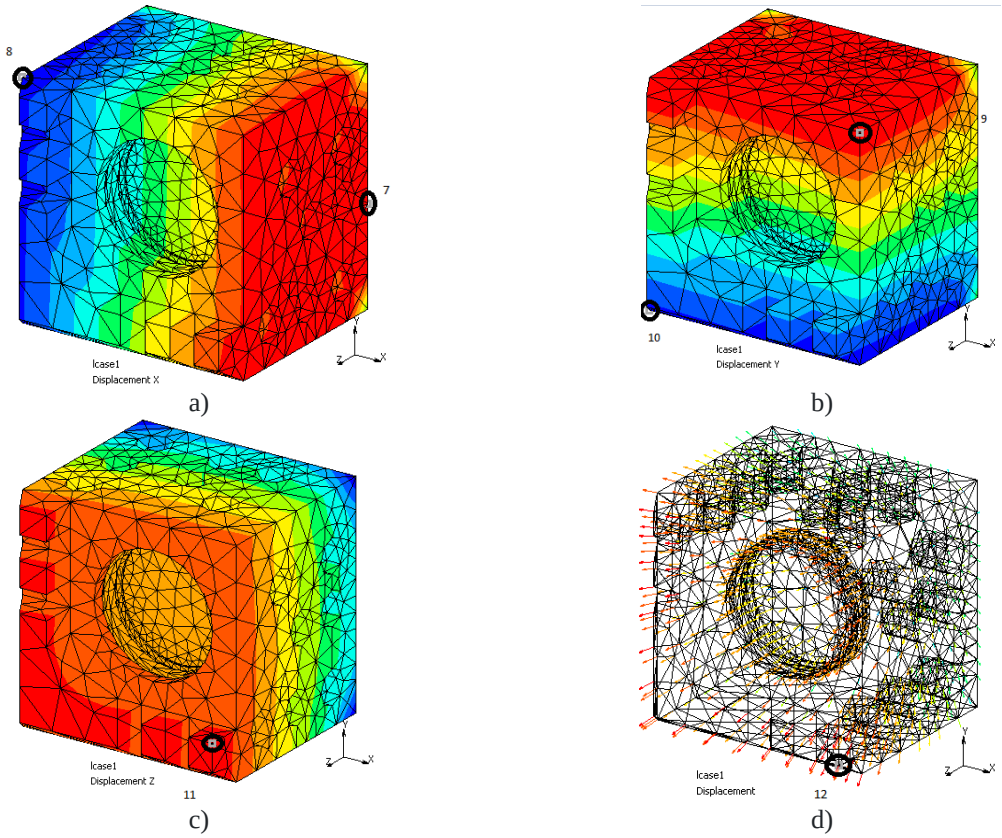

Fig. 4. – The displacement of the second model made of AlMgSi1 under simulation: a) x-direction, b) y-direction displacement, c) z-direction displacement, d) total displacement

Fig. 6 shows the spectrum of displacements.

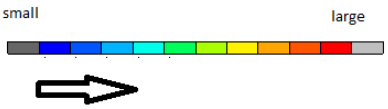

Fig. 5. – Spectrum of displacements

As the coordinate axes located at the center and bottom of the workpiece on XY plane, the displacement in X and Y direction had both sign while Z-direction ad total displacement only had positives sign. Table 2-4 recorded the largest value of 4 types of displacements at the highest temperature (22.45°C) and Fig. 5 and Fig. 6 illustrated the position having those values.

Several conclusions could be drawn for the first phase of simulation:

- In x and y direction, the displacement is the lowest at the middle of the model and larger when reach edges;
- In z direction, the displacement is the lowest at the bottom and is the highest at the top of the model;
- The displacement in z direction dominated the maximum value of total displacement;
- The node has the maximum displacement in total will be at the max value point of z displacement or near that PMMA has larger expansion coefficient so that the displacement is significant bigger than the two rest cases (Aluminum and AlMgSi1 have similar expansion coefficients).

In [11,12], the first model's dimensional parameters were measured including length and width of 5 rectangles and the height. To compensate for the change of temperature, Eq. (5) was used and the average temperature for whole process was assumed to be 21.9°C with PMMA and 22.3°C with Al. With the simulation, value of displacements was recorded at the same temperature. The Eq. (6) illustrates how to calculated the distance between two points A (x_A, y_A, z_A) and B (x_B, y_B, z_B) which have the displacement respectively in direction x, y and z $\boldsymbol{\Delta}$A $(\Delta x_A, \Delta y_A, \Delta z_A)$ and $\boldsymbol{\Delta}$B $(\Delta x_B, \Delta y_B, \Delta z_B)$:

$$ND(new\ distance) = \sqrt{(x_A + \Delta x_A - x_B - \Delta x_B)^2 + (y_A + \Delta y_A - y_B - \Delta y_B)^2 + (z_A + \Delta z_A - z_B - \Delta z_B)^2} \quad (6)$$

$$OD(original\ distance) = \sqrt{(x_A - x_B)^2 + (y_A - y_B)^2 + (z_A - z_B)^2} \quad (7)$$

$$ME(measurement\ error) = ND - OD \quad (8)$$

Applying the above equation, Table 5 compare the corrected value used in [11,12] and the corrected value calculated by simulation.

Table 5. Comparison between corrected values between using Eq.(3) and simulations

Dimensional parameters	*Corrected values by equations [μm]*		*Corrected values by simulations [μm]*	
	PMMA	Al	PMMA	Al
Width	5	1	5.208	1.360
Length	10	2	9.748	2.331
Heigh	14	3	15.66	4.127

The deviations between corrected values are normally smaller than 1 μm which can be considered neglectable. On the other hand, the results of Eq. (5) are usually smaller than from the simulations.

Conclusions

With installed cooling systems, computed tomography is expected to maintain ideal temperature during the process of measurement. However, the expectation cannot be fulfilled, which was proved in [11,12] with the change of temperature. Consequently, measurement errors caused by thermal expansion are inevitable. The simulation of temperature change's effect was implemented on 2 models with different materials where thermal expansion coefficients are distinctive to reveal the possible errors.

With Marc Mentat and FEM method, the distribution of displacement in whole body of specimens were illustrated. It was also proved that maximum displacements for aluminum material is under 5 μm and for PMMA is under 20 μm for both models. In previous work, corrected values were calculated by Eq. (5) to compensate the change in temperature, which was compared with the value from the simulation. With the deviation under 1 μm, it can be concluded that using Eq. (5) to calculate compensated value if temperature during CT process cannot be maintained at 20 °C is applicable to simplify the work of determining the results of measurement.

References

[1] Villarraga-Gómez, H., Morse, E. P., Hocken, R. J., & Smith, S. T. (2014). Dimensional metrology of internal features with X-ray computed tomography // Proc. of 29th ASPE Annual meeting, 2014, P. 684-689.

[2] Reinhart, C. (2008, October). Industrial computer tomography–a universal inspection tool. In 17th world conference on nondestructive testing, P. 25-28.

[3] Kruth, J. P., Bartscher, M., Carmignato, S., Schmitt, R., De Chiffre, L., & Weckenmann, A. (2011). Computed tomography for dimensional metrology. CIRP annals, 60(2), P. 821-842.

[4] Welkenhuyzen, F., Kiekens, K., Pierlet, M., Dewulf, W., Bleys, P., Kruth, J. P., & Voet, A. (2009). Industrial computer tomography for dimensional metrology: Overview of influence factors and improvement strategies. In Proceedings of the 4th international conference on optical measurement techniques for structures and systems: Optimess 2009, P. 401-410.

[5] Hiller, J., Maisl, M., & Reindl, L. M. (2012). Physical characterization and performance evaluation of an x-ray micro-computed tomography system for dimensional metrology applications. Measurement Science and Technology, 23(8), 085404.

[6] Drégelyi-Kiss, Á. (2019, June). Towards Traceable Dimensional Measurements by Micro Computed Tomography. In International Conference on Measurement and Quality Control-Cyber Physical Issue (pp. 247-254). Springer, Cham

[7] Dao, A., & Drégelyi-Kiss, Á. (2020). Determination of GD&T Features Varying the Setting Parameters of X-Ray Computed Tomography by Response Surface Method. In Materials Science Forum (Vol. 994, pp. 280-287). Trans Tech Publications Ltd.

[8] Aloisi, V., & Carmignato, S. (2016). Influence of surface roughness on X-ray computed tomography dimensional measurements of additive manufactured parts. Case studies in nondestructive testing and evaluation, 6, 104-110

[9] Villarraga, H., Morse, E., Hocken, R., & Smith, S. (2014). A study on material influences in dimensional computed tomography. In Proceedings–ASPE 2014 annual meeting (pp. 67-72).

[10] Su, S., Dai, N., Cheng, X., Zhou, X., Wang, L., & Villarraga-Gómez, H. (2019). A Study on Factors Influencing the Accuracy Evaluation of Dimensional X-Ray Computed Tomography with Multi-sphere Standards. International Journal of Precision Engineering and Manufacturing, 1-13.

[11] Villarraga-Gómez, H., Thousand, J. D., Morse, E. P., & Smith, S. T. (2015). CT measurements and their estimated uncertainty: The significance of temperature and bias determination. In ASPE Mets & Props, 60, J. Phys.: Conf. Ser.

[12] Villarraga-Gómez, H., Thousand, J. D., & Smith, S. T. (2020). Empirical approaches to uncertainty analysis of X-ray computed tomography measurements: A review with examples. Precision Engineering, 64, 249-268.

[13] Bartscher, M., Illemann, J., & Neuschaefer-Rube, U. (2016). ISO test survey on material influence in dimensional computed tomography. Case studies in nondestructive testing and evaluation, 6, 79-92.

[14] Wenig, P., & Kasperl, S. (2006, September). Examination of the measurement uncertainty on dimensional measurements by X-ray computed tomography. In Proceedings of 9th European Conference on Non-Destructive Testing (ECNDT), Berlin, Germany.

[15] Drégelyi-Kiss, Á., & Durakbasa, N. M. (2018, August). Measurement error on the reconstruction step in case of industrial computed tomograph. In The International Symposium for Production Research (pp. 309-323). Springer, Cham.

[16] Bartscher, M., Sato, O., Härtig, F., & Neuschaefer-Rube, U. (2014). Current state of standardization in the field of dimensional computed tomography. Measurement Science and Technology, 25(6), 064013.

[17] Hiller, J., Fuchs, T. O., Kasperl, S., & Reindl, L. M. (2011). Influence of the quality of X-ray computed tomography image on coordinate measurements. Principles, measurements and simulations. TM. Technisches Messen, 78(7-8), 334-347.

[18] Villarraga-Gómez, H., Lee, C., & Smith, S. T. (2018). Dimensional metrology with X-ray CT: A comparison with CMM measurements on internal features and compliant structures. Precision Engineering, 51, 291-307.

[19] Therefore, S. T. C., & AS, M. (1993). Guide to the Expression of Uncertainty in Measurement.

[20] ISO 15530-3 (2011), Geometrical product specifications (GPS)-Coordinate measuring machines (CMM): Technique for determining the uncertainty of measurement -Part 3: Use of calibrated workpieces or measure standards, Geneva (Switzerland): ISO copyright office.

Information of the authors

Ágota Drégelyi-Kiss, associate professor, Óbuda University, Budapest, Hungary
e-mail: dregelyi.agota@bgk.uni-obuda.hu

Anh Dao Duy, PhD student, Óbuda University, Budapest, Hungary
e-mail: duyanhbmehust@gmail.com

Farkas Gabriella, PhD, associate professor, Óbuda University, Budapest, Hungary
e-mail: farkas.gabriella@bgk.uni-obuda.hu

Viktor Gonda, associate professor, Óbuda University, Budapest, Hungary, corresponding author
e-mail: gonda.viktor@bgk.uni-obuda.hu